

## Full Paper

# Preparation, Characterization, and Electrocatalytic Properties of Cobalt Oxide and Cobalt Hexacyanoferrate Hybrid Films

Shen-Ming Chen,\* Ming-Huei Wu, R. Thangamuthu

Department of Chemical Engineering and Biotechnology, National Taipei University of Technology, No. 1, Section 3, Chung-Hsiao East Road, Taipei, 106 Taiwan

\*e-mail: smchen78@ms15.hinet.net

Received: June 18, 2007

Accepted: September 20, 2007

## Abstract

Polynuclear mixed-valent films of cobalt oxide and cobalt hexacyanoferrate (CoOCoHCF) have been deposited on electrode surfaces from a solution of  $\text{Co}^{2+}$  and  $\text{Fe}(\text{CN})_6^{3-}$  ions by repetitive potential cycling method. Simultaneous cyclic voltammetry and electrochemical quartz crystal microbalance measurements demonstrate the steady growth of modified film. The effect of type of monovalent cations as well as acidity of the supporting electrolyte on film growth and redox behavior of resulting film was investigated. In pure supporting electrolyte, electrochemical responses of modified electrode resemble with that of a surface immobilized redox couple. The hybrid film electrodes showed electrocatalytic activity toward oxidation of NADH, hydrazine and hydroxylamine. The feasibility of using our modified electrodes for analytical application was also explored.

**Keywords:** Cobalt oxide, Cobalt hexacyanoferrate, Hybrid film, Modified electrode, Electrocatalysis

DOI: 10.1002/elan.200704036

## 1. Introduction

Metal hexacyanoferrates are an important class of insoluble mixed-valence polynuclear compounds extensively used to prepare chemically modified electrodes (CMEs) [1–12]. Because they can produce well characterized electroactive films with properties in common not only with redox and ion-exchange polymers but also with intercalation compounds. Studies on metal hexacyanoferrates have mainly been focused on transition metal compounds including Prussian blue [1], cadmium hexacyanoferrate (CdHCF) [2], zinc hexacyanoferrate (ZnHCF) [3], copper hexacyanoferrate (CuHCF) [4], cobalt hexacyanoferrate (CoHCF) [5], nickel hexacyanoferrate (NiHCF) [6], indium hexacyanoferrate (InHCF) [7], vanadium hexacyanoferrate (VHCF) [8], lanthanum hexacyanoferrate (LaHCF) [9], palladium hexacyanoferrate (PdHCF) [10], manganese hexacyanoferrate (MnHCF) [11], and also hybrid hexacyanoferrates, for example copper and cobalt hexacyanoferrate (CuCoHCF) [12]. The electrode surfaces can be modified with metal hexacyanoferrate by different ways such as electrodeposition, adsorption, entrapping into a polymer matrix, electrodeless deposition, mechanically attaching the insoluble metal-hexacyanoferrate or by the reaction between metal hexacyanoferrate with self-assembled monolayer of an organosulfur compound on a gold electrode [13–18].

Among the transition metal hexacyanoferrates, cobalt hexacyanoferrate is considered as attractive material to modify the electrode surfaces due to its excellent reversible redox behavior [19, 20]. The structure and electrochemical

properties of CoHCF have been reported in the literature [21, 22]. Recently, with the microdialysis sampling technique, morphine was detected in rat brain by using HPLC on a cobalt hexacyanoferrate chemically modified electrode [23]. Cobalt hexacyanoferrate-modified glassy carbon electrodes have also been shown to be useful for electrocatalytic oxidation of NADH [14], ascorbic acid [22], dopamine [19] and hydrazine [24]. Cobalt, nickel and indium hexacyanoferrate films have shown catalytic activity towards electro-oxidation of  $\text{SO}_2^{3-}$  and  $\text{S}_2\text{O}_3^{2-}$  ions [7].

In continuation of our study to prepare modified electrodes using metal hexacyanoferrates [5, 7, 25–27], in the present study, we have prepared mixed cobalt oxide cobalt hexacyanoferrate (CoOCoHCF) hybrid film modified electrodes. The film growth, surface morphology and electrochemical properties of the modified electrodes were investigated. Finally, the electrocatalytic activity of CoOCoHCF hybrid film modified electrodes toward NADH, hydrazine and hydroxylamine oxidation were tested. To evaluate the utility of our modified electrodes for analytical application, they have been used for amperometric determination of hydrazine and hydroxylamine. In addition to this, the modified electrode was used for monitoring hydroxylamine in flowing stream.

## 2. Experimental

All the chemicals used were of analytical grade and used without further purification. The aqueous solutions were

prepared using doubly distilled deionized water and then deaerated by purging with high purity nitrogen gas for about 20 min before performing electrochemical experiments. Also, a continuous flow of nitrogen over the aqueous solution was maintained during measurements.

The electrochemical experiments were carried out with a CH Instruments (Model CHI-400) using CHI-750 potentiostat. Cyclic voltammograms were recorded in a three-electrode cell configuration, in which a BAS glassy carbon electrode (area = 0.07 cm<sup>2</sup>). The auxiliary compartment contained a platinum wire that was separated by a medium-sized glass frit. Cell potentials were recorded using an Ag | AgCl | KCl (saturated solution) electrode. The working electrode for electrochemical quartz crystal microbalance (EQCM) measurements was an 8 MHz AT-cut quartz crystal with gold coating.

Amperometric experiments were performed using PINE Instrument (USA) in conjunction with CHI-750 potentiostat connected to a Model AFMSRX analytical rotator. Flow injection analysis system consisted of a carrier reservoir, a Cole Parmer Masterflex microprocessor pump drive, a Rehodyne 7125 sample injection valve (20- $\mu$ L loop), interconnecting Teflon tubing, and a BAS CC-5 type electrochemical injector (West Lafayette, IN). The flow injection analysis was carried out at an applied potential of +0.6 V (vs. Ag/AgCl). The flow rate was 1.5 mL min<sup>-1</sup>. Note that screen-printed electrode (SPE) with a working area of 0.196 cm<sup>2</sup> purchased from Zensor R&D (Taichung, Taiwan), was used as working electrode in FIA. The SPE was modified with CoOCoHCF hybrid film by adopting similar procedure used to modify GCE. HITACHI Model S-3000H scanning electron microscope was used for surface analysis of the modified electrodes. CSPM 4000 (Ben Yuan Ltd, China) scanning Probe Microscope was used to record AFM images in tapping mode.

Prior to film deposition, the glassy carbon electrode (GCE) was polished with 0.05  $\mu$ m alumina on Buehler felt pads and then ultrasonically cleaned for about a minute in water. Finally, the electrode was washed thoroughly with double distilled water and used. The electrochemical deposition of CoOCoHCF hybrid films was accomplished by potentiodynamic cycling of the working electrode between pre-set potential range in a suitable aqueous solution containing Co<sup>2+</sup> and Fe(CN)<sub>6</sub><sup>3-</sup> ions. After film formation, the electrode was rinsed with distilled water and used for further investigation.

### 3. Results and Discussion

#### 3.1. Preparation of Mixed Cobalt Oxide and Cobalt Hexacyanoferrate Film Modified Electrodes

Figure 1 illustrates repetitive cyclic voltammograms recorded during electrodeposition of cobalt oxide and cobalt(II) hexacyanoferrate hybrid film on GC electrode from aqueous solution of 0.1 M BaCl<sub>2</sub> (pH 6.5) containing Co<sup>2+</sup> and Fe(CN)<sub>6</sub><sup>3-</sup> ions. The progressive increase of both anodic and

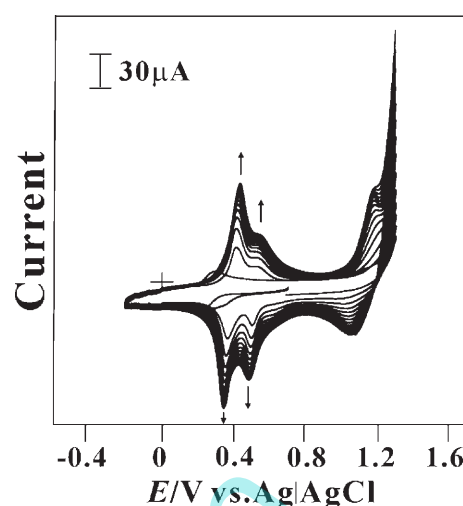


Fig. 1. Repeated cyclic voltammograms of CoOCoHCF hybrid film growth on GCE from the aqueous solution of 0.1 M BaCl<sub>2</sub> (pH 6.5) containing 1  $\times$  10<sup>-3</sup> M Co<sup>2+</sup> and 1  $\times$  10<sup>-3</sup> M Fe(CN)<sub>6</sub><sup>3-</sup>. Scan rate = 0.1 V s<sup>-1</sup>.

cathodic peak currents demonstrates continuous deposition of CoOCoHCF hybrid film on GC electrode surface. It can be seen that there are three redox couples present in all voltammograms with formal potentials occurring at about 0.37, 0.50, and 1.15 V (vs. Ag | AgCl). Among these, the redox couples correspond to the formal potential of 0.37 and 0.50 V (vs. Ag | AgCl) were attributed to cobalt (II) hexacyanoferrate film while the third one at 1.15 V was attributed to originate from the redox transition of cobalt oxide.

Figures 2 and 3 illustrate effect of type of monovalent cation (Na<sup>+</sup> or K<sup>+</sup>) as well as pH of supporting electrolyte on formation and electrochemical characteristics of CoO-CoHCF hybrid film. In neutral and acidic solutions, only the redox couple and the formal potential of the cobalt(II) hexacyanoferrate occurring at the potential about +0.4 V (vs. Ag | AgCl) showed a dependency on the monovalent cation of supporting electrolyte. On the other hand, the most positive formal potential corresponding to cobalt oxide redox transition was affected in weak basic solutions due to changes in monovalent cation of electrolyte.

#### 3.2. In Situ EQCM Study of CoOCoHCF Hybrid Film Growth

In order to study the growth of CoOCoHCF film, we have performed simultaneous voltammetric and microgravimetric experiments. Simultaneous cyclic voltammetry and electrochemical quartz crystal microbalance measurements permit continuous monitoring of surface mass changes without disturbing experimental conditions. Figures 4A and B show cyclic voltammograms and simultaneously recorded microgravimetric spectrograms of CoOCoHCF hybrid film on gold electrode prepared from 0.1 M CH<sub>3</sub>COONa solution (pH 8.6) containing 1 mM of Fe(CN)<sub>6</sub><sup>3-</sup> and Co<sup>2+</sup>. It is

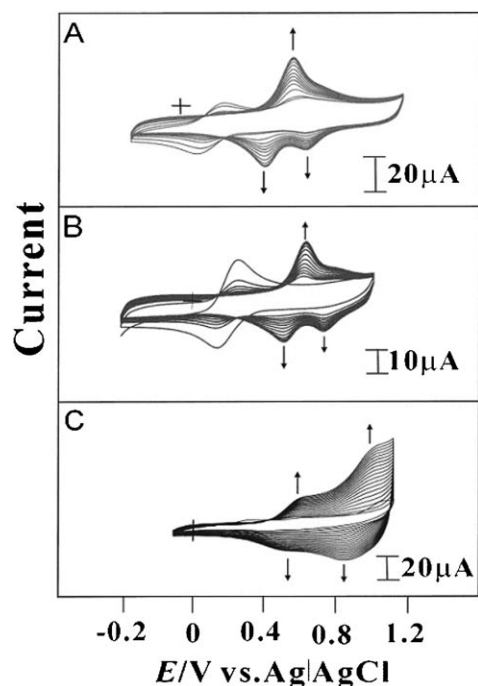


Fig. 2. Repeated cyclic voltammograms of CoOCoHCF hybrid film growth on GCE from the aqueous solution of different pH containing  $1 \times 10^{-3}$  M  $\text{Co}^{2+}$ ,  $1 \times 10^{-3}$  M  $\text{Fe}(\text{CN})_6^{3-}$  and 0.5 M KCl. A) pH 5; B) pH 7; and C) pH 10. Scan rate =  $0.1 \text{ V s}^{-1}$ .

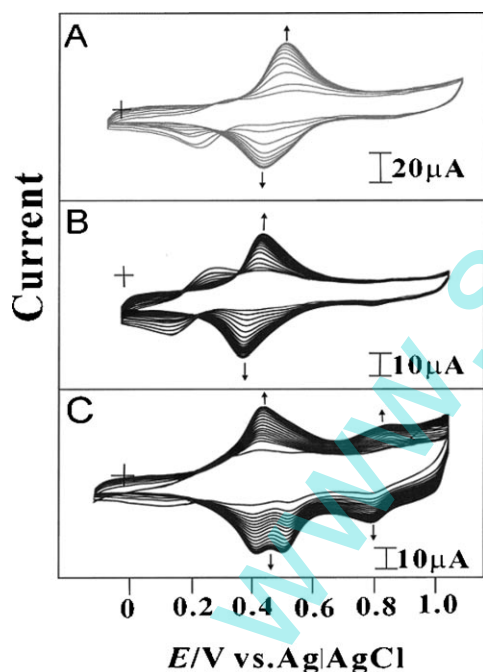


Fig. 3. Repeated cyclic voltammograms of CoOCoHCF hybrid film growth on GCE from the aqueous solution of different pH containing  $1 \times 10^{-3}$  M  $\text{Co}^{2+}$ ,  $1 \times 10^{-3}$  M  $\text{Fe}(\text{CN})_6^{3-}$  and 0.5 M NaCl. A) pH 5.5; B) pH 7; and C) pH 9. Scan rate =  $0.1 \text{ V s}^{-1}$ .

obvious that peak current in cyclic voltammograms increases with scanning number, while frequency decreases during microgravimetric measurement. According to Sauerbrey

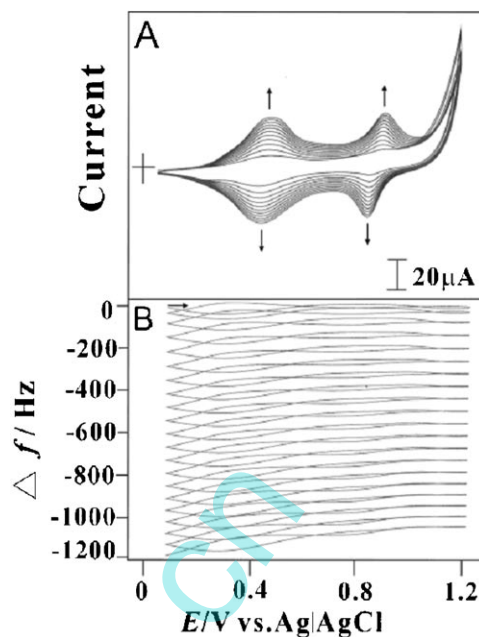
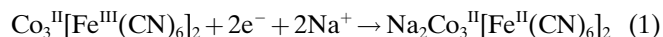


Fig. 4. A) Repeated cyclic voltammograms of CoOCoHCF hybrid film growth on a gold electrode from the aqueous solution containing  $1 \times 10^{-3}$  M  $\text{Co}^{2+}$ ,  $1 \times 10^{-3}$  M  $\text{Fe}(\text{CN})_6^{3-}$  and 0.1 M  $\text{CH}_3\text{COONa}$  (pH 8.6). Scan rate =  $0.02 \text{ V s}^{-1}$ . B) Change in the EQCM frequency recorded concurrently with the first five repeated CVs between the potentials of 0.1 and 1.2 V.

equation [28], frequency drop corresponds to mass gain. It is evident from the analysis of EQCM responses that deposition of cobalt (II) hexacyanoferrate occurred between 0.4–0.8 V (vs. Ag|AgCl) whereas deposition of cobalt oxide occurred between the potential range of 0.8–1.1 V (vs. Ag|AgCl). The results also demonstrate that CoOCoHCF hybrid film grows steadily with time.

The cyclic voltammograms of CoOCoHCF hybrid film showed two sets of redox peaks. The first redox transition occurs with a formal potential of +0.48 V and the other at +0.89 V. The corresponding redox reactions are represented as follows [20]:



The second peak at +0.89 V in Figure 4 appears only when the anodic switching potential is extended up to 1.0 V. Tacconi et al. [29] have assigned this feature to  $\text{Co}^{2+}/\text{Co}^{3+}$  oxidation process based on control voltammetry data acquired in the absence of  $\text{Fe}(\text{CN})_6^{3-}$ . Thus, the second redox couple with a formal potential of +0.89 V appearing in Figure 4 can be ascribed to redox transition of cobalt oxide.

In the EQCM experiments, change in mass at quartz crystal was calculated from the change in frequency using Sauerbrey equation [28]

$$\text{Mass change } (\Delta m) = (-1/2)(f_0^{-2})(\Delta f) A (kq)^{1/2} \quad (2)$$

Where,  $A$  is the area of the gold disk coated onto the quartz crystal,  $\rho$  is the density of the crystal,  $k$  is the shear modulus

of the crystal,  $\Delta f$  is the measured frequency change, and  $f_0$  is the oscillation frequency of the crystal. A frequency change of 1 Hz is equivalent to a 1.4 ng change in mass. The relatively small mass of CoOCoHCF hybrid film that deposited during the first two scans was reflecting the difficulties occurred initially in adherence of film on clean gold electrode surface. Later, the rate of film growth was faster compared to first two scans as shown in Figure 4 B. In the present study, about  $8500 \text{ ng cm}^{-2}$  of CoOCoHCF hybrid film was deposited on gold electrode after twenty cyclic voltammetric scans.

### 3.3. Surface Characterization of CoOCoHCF Hybrid Films

The morphology of CoOCoHCF films was investigated using scanning electron microscope (SEM). Figure 5A shows SEM image of a thin film of CoOCoHCF electrodeposited from 0.1 M  $\text{CH}_3\text{COONa}$  aqueous solution (pH 8.6) containing  $\text{Co}^{2+}$  and  $\text{Fe}(\text{CN})_6^{3-}$  ions on indium tin oxide (ITO) coated glass surface. The SEM studies of iron hexacyanoferrate (PB) also showed that electrosynthesized films have a nonuniform structure with an average grain size in the range of 110 to 450 nm [30, 31]. However, the SEM micrograph of CoOCoHCF film indicates existence of distinguished individual crystallites. Films of such a structure are known to have existed only for cadmium hexacyanoferrate, which has a lower-symmetry orthorhombic lattice [2].

The SEM micrograph of CoOCoHCF film prepared from acidic condition (pH 4) is shown in Figure 5B. The morphology shows that a thin porous film of cobalt hexacyanoferrate is formed, in which cobalt oxide particles with a flower like columnar structure is scattered. The SEM investigation by Wollenstein et al. [32] showed that cobalt oxide film is polycrystalline with columnar grown grains as observed in the present study.

The surface morphology of CoOCoHCF hybrid film was also examined with atomic force microscopy (AFM). A typical three-dimensional AFM image of electrodeposited thin film on ITO electrode is shown in Figure 5C. The film was obtained from 0.1 M  $\text{CH}_3\text{COONa}$  aqueous solution (pH 8.6) containing  $\text{Co}^{2+}$  and  $\text{Fe}(\text{CN})_6^{3-}$  ions. It can be noticed from the micrograph that grain features are protruding from the film surface. The maximum thickness of the film was estimated to be 746 nm.

### 3.4. The Electrochemical Characteristics of CoOCoHCF Hybrid Film Modified Electrodes

Figure 5D shows cyclic voltammetric responses of CoOCoHCF hybrid film modified electrodes in 0.1 M  $\text{BaCl}_2$  solution (pH 6.5) at various scan rates over 10–200  $\text{mV s}^{-1}$  range. The anodic and cathodic peak currents are directly proportional to scan rate as shown in the inset for the first well-defined redox couple. The ratio of anodic to cathodic

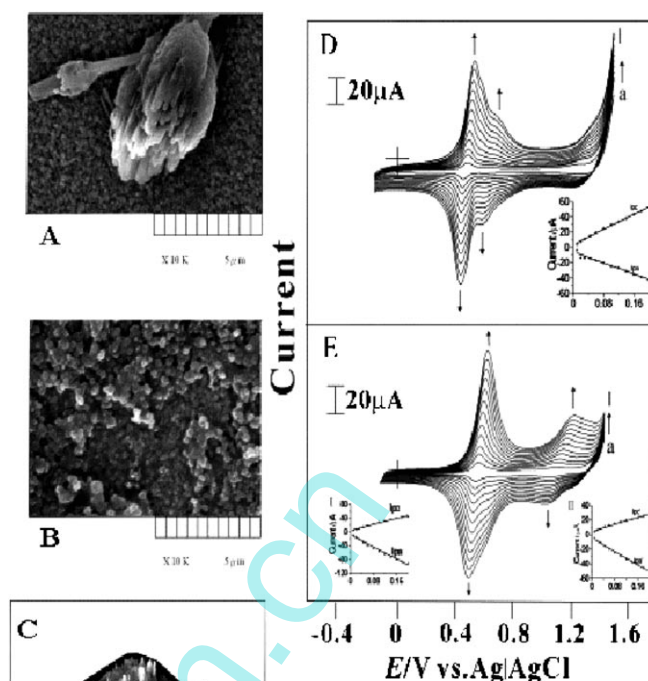


Fig. 5. A) and B) SEM photograph of CoOCoHCF hybrid film deposited on ITO electrode from 0.1 M  $\text{CH}_3\text{COONa}$  aqueous solution containing  $1 \times 10^{-3} \text{ M Co}^{2+} + 1 \times 10^{-3} \text{ M Fe}(\text{CN})_6^{3-}$  at pH 8.6 and 4, respectively. C) Three dimensional AFM image of CoOCoHCF hybrid film prepared at pH 8.6. D) and E) Repeated cyclic voltammograms of GCE modified with CoOCoHCF hybrid film at different scan rates: a) 0.01; b) 0.02; c) 0.03; d) 0.045; e) 0.06; f) 0.08; g) 0.1; h) 0.12; i) 0.14; j) 0.16; k) 0.18; and l) 0.2  $\text{V s}^{-1}$  in 0.1 M  $\text{BaCl}_2$  aqueous solution of pH 6.5 and 0.1 M  $\text{CH}_3\text{COONa}$  aqueous solution of pH 8.6, respectively. Insets show variation of anodic peak current ( $I_{pa}$ ) and cathodic peak current ( $I_{pc}$ ) with scan rate.

peak currents, i.e.,  $i_{pa}/i_{pc}$ , was almost unity. These observations indicated that the redox process was confined to the surface of the CoOCoHCF hybrid film on glassy carbon electrode, confirming the immobilized state of the hybrid cobalt oxide and cobalt (II) hexacyanoferrate. The behavior of CoOCoHCF hybrid film modified electrode is essentially the same electrochemical characteristics as that of Prussian blue analogues [33]. For the modified film with such characteristics, the peak current and scan rate are related as follows [34]:

$$I_p = n^2 F^2 \nu A \Gamma_0 / 4RT \quad (3)$$

where,  $\Gamma_0$ ,  $\nu$ ,  $A$ , and  $I_p$  represent the surface coverage, scan rate, electrode area, and peak current, respectively.

Similarly, the cyclic voltammetric responses of CoO-CoHCF hybrid film modified electrodes in 0.1 M CH<sub>3</sub>COONa (pH 8.6) is shown in Figure 5E. As in the previous case, the anodic and cathodic peak currents show a close linear dependence on scan rate for both the well-defined as well as the ill-defined redox couples. This behavior again demonstrates the surface-confined charge transfer characteristic of CoOCoHCF hybrid film.

### 3.5. Electrocatalytic Behavior of CoOCoHCF Hybrid Film Towards Oxidation of NADH, Hydrazine and Hydroxylamine

Electrocatalytic behavior of CoOCoHCF hybrid film modified electrode towards oxidation of NADH, hydrazine and hydroxylamine was investigated using cyclic voltammetry.

Figure 6A shows cyclic voltammetric responses of CoO-CoHCF hybrid film modified electrode (a–f) in 0.1 M LiCl (pH 6.5) containing different concentrations of NADH varying from 0 to 1.5 mM. It can be seen that the anodic peak current increases with increasing NADH concentration. In this figure, cyclic voltammogram, a', corresponds to the response of 1.5 mM NADH oxidation at unmodified GC electrode. Comparison of voltammograms, a', and, f, clearly indicates that the CoOCoHCF hybrid film catalyzes the oxidation of NADH. As this figure shows, anodic peak potential of NADH oxidation on CoOCoHCF hybrid film modified electrode is much lower than that of unmodified electrode. In other words, a decrease in overpotential can be

observed with modified electrode. As the catalytic peak occurred near the formal potential of cobalt hexacyanoferrate redox couple, it is reasonable to ascribe that this redox couple catalyzed NADH oxidation.

Figure 6B shows cyclic voltammograms of CoOCoHCF hybrid film modified electrode in 0.1 M CH<sub>3</sub>COONa solution of pH 8 (a) and in the presence of different concentration of hydrazine (b–d), and also the response of bare electrode (a') for 3 mM hydrazine. Similar experimental results were obtained for hydroxylamine and shown in Figure 6C. In both cases, the anodic peak current increases with increasing substrate concentration. Also, there were no appreciable oxidation occurred at unmodified electrode. In the case of hydrazine, electrocatalytic activity was attributed to the cobalt hexacyanoferrate redox couple while different situation prevailed in hydroxylamine. Here, both cobalt hexacyanoferrate as well as cobalt oxide redox couples are responsible for the catalysis.

It is worthy to mention here that CoOCoHCF hybrid film coated electrode catalyzes efficiently the oxidation of all the three substrates studied above in terms of current, i.e., the catalytic process is mainly contributed by the current height rather than decreasing oxidation potential drastically [35]. Although this factor may limit the potentiality of present modified electrode to some extent, but still it has several advantages compared to bare electrode. For example, a decrease in overpotential can be observed for all the substrates investigated. In particular, in the case of hydrazine and hydroxylamine, no appreciable oxidation was noticed at unmodified electrode.

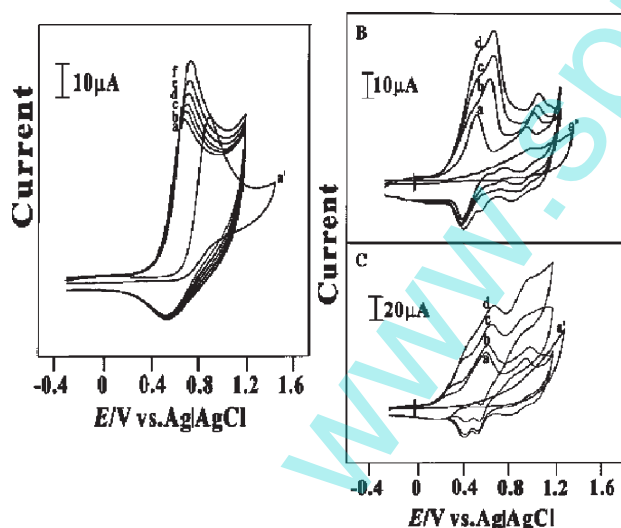


Fig. 6. Cyclic voltammograms of GCE modified with CoO-CoHCF hybrid film in: A) 0.1 M LiCl (pH 6.5) containing different concentrations of NADH: a) 0; b)  $5 \times 10^{-4}$ ; c)  $1 \times 10^{-3}$ ; d)  $1.5 \times 10^{-3}$ ; e)  $2 \times 10^{-3}$ ; and f)  $2.5 \times 10^{-3}$  M; B) and C) in 0.1 M CH<sub>3</sub>COONa (pH 8) containing different concentrations of N<sub>2</sub>H<sub>4</sub> and NH<sub>2</sub>OH, respectively: a) 0; b)  $1 \times 10^{-4}$ ; c)  $2 \times 10^{-4}$ ; d)  $3 \times 10^{-4}$  M. Curve a' in A, B and C corresponds to oxidation of  $2.5 \times 10^{-3}$  M NADH,  $3 \times 10^{-4}$  M N<sub>2</sub>H<sub>4</sub> and NH<sub>2</sub>OH, respectively on unmodified GC electrode. Scan rate = 0.1 V s<sup>-1</sup>.

### 3.6. Analytical Application of CoOCoHCF Hybrid Film Modified Electrodes

#### 3.6.1. Constant Potential Amperometry in Stirred Solution

The determination of hydrazine and hydroxylamine at the CoOCoHCF hybrid film modified electrode was carried out using standard addition method. For comparison similar experiments were also performed with unmodified electrode.

Figure 7A shows typical amperometric current-time response of CoOCoHCF hybrid film modified electrode (b) for successive addition of hydrazine to a continuously stirred solution containing 0.1 M KCl and 0.1 M CH<sub>3</sub>COONa (pH 8). The electrode was held at a potential of 0.6 V (Ag/AgCl) and rotated with a speed of 900 rpm. The amperometric curves are obtained by the successive addition 100 μM of hydrazine. The modified electrode responded rapidly and the catalytic current increases with hydrazine concentration. In the case of bare electrode, current was almost remained unchanged for successive addition because hydrazine not oxidized on it. The calibration curve corresponding to the modified electrode is shown as inset. It can be noticed that the calibration curve is linear in the entire region studied up to 0.9 mM. The modified electrode showed a sensitivity of 38.5 μA μM<sup>-1</sup> with 0.9134 as

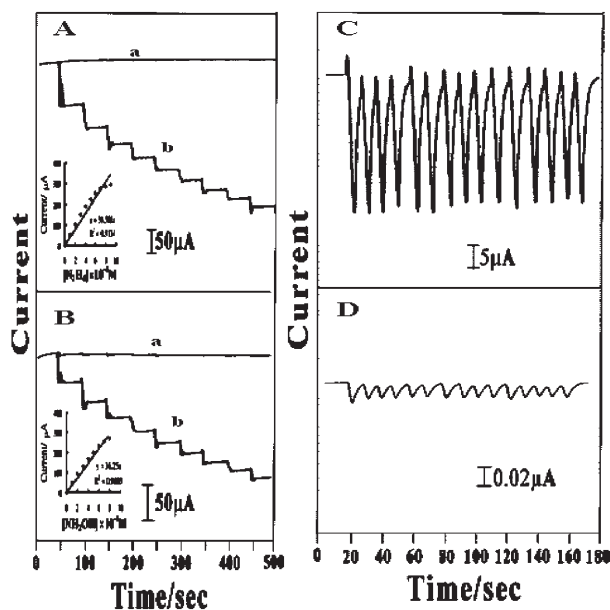


Fig. 7. A) and B) Amperometric responses for the successive addition of  $1 \times 10^{-4}$  M of  $\text{N}_2\text{H}_4$  and  $\text{NH}_2\text{OH}$ , respectively to 0.1 M  $\text{CH}_3\text{COONa}$  (pH 8) containing 0.1 M  $\text{KCl}$ ; applied potential is 0.6 V and the electrode rotation speed = 900 rpm; a) on bare electrode; b) at CoOCoHCF hybrid film modified electrode. C) and D) FIA responses of CoOCoHCF hybrid film modified electrode and bare GCE, respectively for 15 sequential addition of  $\text{NH}_2\text{OH}$  to 0.1 M  $\text{CH}_3\text{COONa}$  (pH 8) buffer solution.  $3 \times 10^{-4}$  M of  $\text{NH}_2\text{OH}$  stock solution was used.

correlation coefficient. Similar measurements were carried out for hydroxylamine. The amperomograms and the calibration curve are presented in Figure 7B. As can be seen, CoOCoHCF hybrid film modified electrode responded rapidly to  $\text{NH}_2\text{OH}$  addition and the steady state was attained within after 10 sec. The linear region in the calibration curve spans up to 0.9 mM with a sensitivity and correlation coefficient of  $36.25 \mu\text{A} \mu\text{M}^{-1}$  and 0.9603, respectively.

### 3.6.2. Flow Injection Analysis

The electrodes modified with CoOCoHCF hybrid film have been tested as amperometric sensors in flowing solutions. In particular, we have investigated hydroxylamine for this purpose. Measurements were conducted in 0.1 M  $\text{CH}_3\text{COONa}$  (pH 8) at an applied potential of 0.6 V (Ag/AgCl). 0.3 mM stock solution was injected with the flow rate of  $1.5 \text{ mL min}^{-1}$ . The flow injection analysis (FIA) results, for 15 sequential additions of hydroxylamine, obtained with CoOCoHCF hybrid film modified and bare electrodes are illustrated in Figures 7C and D respectively. It can be noticed that FIA peaks are well defined, nearly symmetrical for modified electrode compared to poor response of unmodified electrode. The experimental results point that CoOCoHCF hybrid film modified electrodes can be considered useful for the estimation of hydroxylamine in flow stream.

### 3.7. Stability of CoOCoHCF Hybrid Film Modified Electrodes

The stability of the CoOCoHCF hybrid film-modified electrode was evaluated by scanning the electrode potential continuously in pure supporting electrolyte. The peak current of hybrid film-modified electrode was monitored and compared periodically. It was found that the decrease in peak current of CoOCoHCF hybrid film was negligible after long period of continuous cycling, which indicates the present modified electrode was relatively stable. In addition to cyclic voltammetric test, the stability of modified electrode was also evaluated under constant potential mode. Amperometry and FIA results presented in the previous section indicate that the stability of CoOCoHCF hybrid film-modified electrode is indeed satisfactory for analytical applications when operating under constant potential mode.

## 4. Conclusions

The cobalt oxide and cobalt hexacyanoferrate hybrid film modified electrode was successfully prepared by repetitive potential cycling method. The EQCM results showed that deposition of the cobalt (II) hexacyanoferrate film occurred between 0.4–0.1 V (vs. Ag|AgCl) whereas the deposition of cobalt oxide film occurred in the potential range of 0.8–1.1 V (vs. Ag|AgCl). Approximately,  $8500 \text{ ng cm}^{-2}$  of hybrid film was deposited on gold electrode after twenty cyclic voltammetric scans. The SEM morphology analysis of modified layer reveals that a thin porous film of cobalt hexacyanoferrate is formed, in which cobalt oxide with a flower like columnar structure is scattered. In neutral and acidic conditions, redox reaction of cobalt(II) hexacyanoferrate showed a dependency on monovalent cations of supporting electrolyte, while cobalt oxide showed such behavior in weak basic solutions. The electrochemical characterization of modified electrode in pure supporting electrolyte indicated that the redox process was confined to the surface, which confirms the immobilized state of the redox species. The electrocatalytic oxidation of NADH, hydrazine and hydroxylamine on CoOCoHCF hybrid film modified GC electrode was investigated using cyclic voltammetric technique. Finally, analytical application of our modified electrodes was demonstrated by utilizing them in amperometric estimation as well as in flow injection analysis toward determination of hydrazine and hydroxylamine.

## 5. Acknowledgement

This work was financially supported by the National Science Council of Taiwan (ROC).

## 6. References

- [1] W. Hou, E. Wang, *J. Electroanal. Chem.* **1991**, 316, 155.
- [2] C. H. Luangdilok, D. J. Arent, A. B. Bocarsly, R. Wood, *Langmuir* **1992**, 8, 650.
- [3] J. Joseph, H. Gomathi, G. P. Rao, *J. Electroanal. Chem.* **1997**, 431, 231.
- [4] J. Zhou, E. Wang, *Electroanalysis* **1994**, 6, 29.
- [5] S. M. Chen, *Electrochim. Acta* **1998**, 43, 3359.
- [6] B. D. Humphrey, S. Sinka, A. B. Bocarsly, *J. Phys. Chem.* **1987**, 91, 586.
- [7] S. M. Chen, *J. Electroanal. Chem.* **2002**, 521, 29.
- [8] C. W. Liu, S. J. Dong, *Electroanalysis* **1997**, 9, 839.
- [9] S. Q. Liu, H. Y. Chen, *J. Electroanal. Chem.* **2002**, 528, 190.
- [10] M. H. Pournaghi-Azar, H. Dastango, *J. Electroanal. Chem.* **2002**, 523, 26.
- [11] P. Wang, X. Jing, W. Zhang, G. Zhu, *J. Solid State Electrochem.* **2001**, 5, 369.
- [12] X. Cui, L. Hong, X. Lin, *J. Electroanal. Chem.* **2002**, 526, 115.
- [13] Z. Gao, E. Wang, P. Li, Z. Zhao, *Electrochim. Acta* **1991**, 36, 147.
- [14] C. X. Cai, H. Y. Ju, H. Y. Chen, *J. Electroanal. Chem.* **1995**, 397, 185.
- [15] O. Ikeda, H. Yoneyama, *J. Electroanal. Chem.* **1989**, 265, 323.
- [16] M. H. Pournaghi-Azar, H. Razmi-Nerbin, *J. Electroanal. Chem.* **1998**, 456, 83.
- [17] S. Jayarama Reddy, A. Dostal, F. Scholz, *J. Electroanal. Chem.* **1996**, 403, 209.
- [18] J. J. Xu, C. Wang, H. Y. Chen, *Anal. Sci.* **2000**, 16, 231.
- [19] Z. Xun, C. Cai, W. Xing, T. H. Lu, *J. Electroanal. Chem.* **2003**, 545, 19.
- [20] P. J. Kulesza, S. Zamponi, M. A. Malik, M. Berrettoni, A. Wolkiewicz, R. Marassi, *Electrochim. Acta* **1998**, 43, 919.
- [21] O. Sato, Y. Einaga, T. Lyoda, A. Fujishima, K. Hashimoto, *J. Phys. Chem.* **1997**, 101, 3903.
- [22] C. X. Cai, K. H. Xue, S. M. Xu, *J. Electroanal. Chem.* **2000**, 486, 111.
- [23] F. Xu, M. Gao, L. Wang, T. Zhou, L. Jin, J. Jin, *Talanta* **2002**, 58, 427.
- [24] S. M. Golabi, F. Noor-Mohammadi, *J. Solid State Electrochem.* **1998**, 2, 30.
- [25] S. M. Chen, *J. Electroanal. Chem.* **1996**, 401, 147.
- [26] S. M. Chen, C. M. Chan, *J. Electroanal. Chem.* **2003**, 543, 161.
- [27] S. M. Chen, C. J. Liao, V. S. Vasantha, *J. Electroanal. Chem.* **2006**, 589, 15.
- [28] G. Sauerbrey, *Z. Phys.* **1959**, 155, 206.
- [29] N. R. de Tacconi, K. Rajeshwar, R. O. Lezna, *J. Electroanal. Chem.* **2006**, 587, 42.
- [30] P. J. Kulesza, S. Zamponi, M. Berrettoni, R. Marassi, M. A. Malik, *Electrochim. Acta* **1995**, 40, 681.
- [31] D. Ellis, M. Eckhoff, V. D. Neff, *J. Phys. Chem.* **1981**, 85, 1225.
- [32] J. Wollenstein, M. Burgmair, G. Plescher, T. Sulima, J. Hildenbrand, H. Bottner, I. Eisele, *Sens. Actuators B* **2003**, 93, 442.
- [33] K. Itaya, I. Uchida, V. D. Neff, *Acc. Chem. Res.* **1986**, 19, 162.
- [34] R. W. Murray, in *Electroanalytical Chemistry*, Vol. 13 (Ed: A. J. Bard), Marcel Dekker, New York **1983**, p. 191.
- [35] C. P. Anrieux, O. Haas, J.-M. Saveant, *J. Am. Chem. Soc.* **1986**, 108, 8175.